

Investigation of bullet penetration in ballistic gelatin via finite element simulation and experiment[†]

Gil Ho Yoon^{*}, Jun Su Mo, Ki Hyun Kim, Chung Hee Yoon and Nam Hun Lim

School of Mechanical Engineering, Hanyang University, 133-791, Korea

(Manuscript Received October 8, 2014; Revised March 17, 2015; Accepted April 15, 2015)

Abstract

To qualitatively understand the deformation processes and damages in the human body caused by high-speed impact, we conducted experimental and computational investigations for bullet penetration into viscoelastic ballistic gelatin blocks. Because it is difficult to measure the strain rate-dependent material properties of viscoelastic gelatin blocks during high-speed impact, the material properties that are indirectly defined by the stress relaxation test were used for the computational simulation. We also conducted some firing experiments and analyzed the deformation processes of the structures. In particular, the passing through times and the shapes of the temporary and permanent cavities inside the ballistic gelatin blocks were analyzed and compared. This data reveals that the employed material models, with some modifications for the FE simulation, are sufficient for predicting the high-speed impact behaviors. To investigate the shapes of the permanent cavities and fragments made by bullets inside the gelatin blocks, two-dimensional sectional images were taken by an industrial CT scanner and a three-dimensional CAD model was constructed based on these images.

Keywords: Wound ballistics; Ballistic gelatin; Temporary cavity; Permanent cavity; 3-D scanner; Failure model

1. Introduction

This paper conducts research into wound ballistics by experimental and computational approaches. Terminal ballistics is the study of the phenomena that occur when a bullet strikes and penetrates various brittle and ductile objects. When the object is a person or an animal, this is referred to as sophisticated wound ballistics. A firm understanding of the impact of bullets on a human body is important for both improving the survival rate and also for developing efficient ammunition and bullets. To understand wound ballistics, many theoretical and experimental studies have been carried out [1-8]. However, it is still a difficult subject due to the chaotic behavior of high-speed impacts and the various rate-dependent material behaviors [9-12]. From a physical point of view, the most relevant and dominant parameters may be the velocity and deceleration of a projectile as the energy of a projectile is dissipated in terms of its dynamic energy, fracture energy, thermal energy, and sound energy throughout a body caused by a very short impact time. Thus, this study revisits the research on bullet penetration into ballistic gelatin blocks in order to understand the phenomenon experimentally and computationally.

Some relevant research into wound ballistics has been conducted previously [1-8]. Bullet penetration phenomena are

influenced by many factors such as the type of bullet, rotation and traveling speeds of the bullet, and the impact angle. When a bullet penetrates a body, which is a mixture of various materials, the deceleration of a bullet occurs due to the resistance forces of the body. These resistance forces initiate three-dimensional chaotic rotations of the bullet. As expected, the swirling, tumbling, and travelling of a bullet inside a human body causes serious damage. Furthermore, when a bullet hits bone or organs, the resistance forces exhibit sudden changes in magnitude and direction; these forces cause further decelerations and rotations of the bullet. In order to understand these chaotic phenomena, there have been some relevant studies looking into the experimental analysis of ballistic penetration for many materials (e.g., gelatin blocks and soap) [1-8]. In Ref. [13], a ballistic experiment was conducted for double-layered steel plates composed with different materials. A variety of impact conditions, such as the order of layers, nose shape of projectiles, incident angle, and ballistic velocity, were investigated related to the evolution of the perforation mechanisms and failure models of the plates and projectiles. For the nose shape of projectiles, blunt-nosed projectiles and ogival-nosed projectiles were examined. These experiments were conducted with an in-house experimental device for a wide range of projectile velocities above 400 m/s. In Ref. [14], gelatin blocks were shot by spherical steel projectiles with a lower impacting velocity (about 120 m/s). With these low speeds, a projectile

^{*}Corresponding author. Tel.: +82 2 2220 0451

E-mail address: ghy@hanyang.ac.kr, gilho.yoon@gmail.com

[†]Recommended by Associate Editor Jun-Sik Kim

© KSME & Springer 2015

often does not pass through the gelatin block completely. In their research, the topic of interest was the penetration depths versus the velocities normalized by the projectile diameter and the threshold velocity below which passing through does not occur. To identify the effects of various conditions on the penetration depth, some experiments were conducted for different gelatin concentrations, different projectile diameters, and different projectile velocities. In Ref. [15], ballistics with 10% ballistic gelatin blocks behind soft armor were investigated. In their research, the bullet does not penetrate into the gelatin but produces a blunt impact on the gelatin block's surface. Therefore, the attenuation of the shockwave could be monitored using five pressure sensors imbedded at different positions in the gelatin block. In Refs. [16, 17], the expansion behavior of gelatin blocks was investigated. In these studies, projectiles passed through the gelatin blocks completely. In Ref. [16], both the increase in diameter and the length reduction of the temporary expansion cavity in the gelatin block were taken into account. For different gelatin concentrations, lengths of gelatin blocks, and impact velocities, the deformation rates were compared using a set of predefined parameters. In Ref. [17], the passing through of gelatin blocks was investigated using both experiments and numerical simulation. In their research, steel spheres were used as projectiles, and the velocity range of the spherical projectiles was between 728 m/s and 947 m/s. For the simulation case, projectile velocities were increased up to 1630 m/s. In addition, the effect of the instant impact velocity and sphere diameter on the damage of the gelatin blocks was investigated. To validate the effectiveness of their computational model, the test firing findings and the computational results were compared related to the important features of the impact event such as a permanent tunnel formed in the gelatin, the time histories of the pressure at a certain point, and the time histories of the temporary cavity size.

There are some difficulties in studying wound ballistics. One of the challenging issues in understanding wound ballistics is that these events happen for a very short period of time (i.e., about a few microseconds) and that they show chaotic behavior (which is very difficult to reproduce) inside opaque materials such as blood, skin, muscle, and bone. In other words, it is almost impossible to see exactly what happens when a person is hit by a bullet. To cope with this issue, transparent ballistic gelatin blocks (a pseudo-elastic material) or soap (a plastic material), where the internal behavior can be seen and the material properties are similar to those of a human body, are used. To capture the images of fast and large deformations, the use of high-speed cameras is usually adopted. To take snapshots of a bullet travelling faster than Mach 1, several tens of thousands of shots per a second must be taken by a high-speed camera. The speed of a bullet was measured by analyzing the images of a high-speed camera and was determined to be 300 to 400 m/s before impacting the surface of the gelatin block. Due to the resistance forces inside the ballistic gelatin block, the bullet experiences swirling,

yawing, and tumbling once it enters the block, which is also what happens inside of the human body. Another issue that should be considered is the fact that human bodies and bullets usually consist of several heterogeneous materials that exhibit different strengths and failure modes. The failure modes obtained by a standard elongation test are not applicable for the high strain rate deformation case in this scenario because the failure modes can be different. To cope with these difficulties, special experiments must be carried out with some empirical assumptions. Published experimental results can be utilized as in some countries, i.e., the Republic of Korea, and some special licenses can be obtained by administrative governments to test the penetration phenomena for research purposes. Because gelatin blocks with different concentrations can be used, some material properties of the viscoelastic material model are measured for gelatin blocks with different concentrations using a spherical indentation test. In addition, note that by changing the densities of the gelatin blocks (i.e., the ratio between the gelatin powder and water), it is possible to make gelatin blocks with material properties and fracture mechanisms that are similar to those of a human body. Depending on the subjects of each study, the densities studied for bullet penetration can vary. In this study, 10% gelatin blocks are made at a low temperature (between 0 °C and 10 °C). Finally, obtaining physically meaningful numerical simulation for the penetration phenomena for a very short period of time inside of a rate-dependent, nonlinear material is still a challenging task. In our study, we simulate ballistic gelatin blocks with embedded bone and nerve fiber and conduct real firing tests in order to show the validity of our simulations and to understand the physical behaviors of the gelatin blocks. For the FE simulation, the Equation of state (EOS), Johnson-Cook failure model, and viscoelastic material model are employed for the simulation of the bullet and gelatin. Some material properties published in the literature are also employed.

The layout of this paper is organized as follows: the material failure models and the material properties are briefly discussed in Sec. 2; some finite element simulations are also conducted. In Sec. 3, gun firing tests, using the same simulation conditions of Sec. 2, are carried out and their results are compared. The conclusion section summarizes our findings and presents some future research topics.

2. Finite element simulation of high-speed impact of gelatin block

Among the four sub-areas of ballistics, i.e., interior ballistics, intermediate ballistics, exterior ballistics, and terminal ballistics, this research is interested in terminal ballistics, which studies the penetration of a target (simulating a body) by a bullet. Compared with the times of the first three ballistic sub-areas, terminal ballistics takes the longest time. Therefore, it is challenging to computationally analyze the behavior of a promptly deformed structure and many numerical and experimental approaches have been previously developed [16–

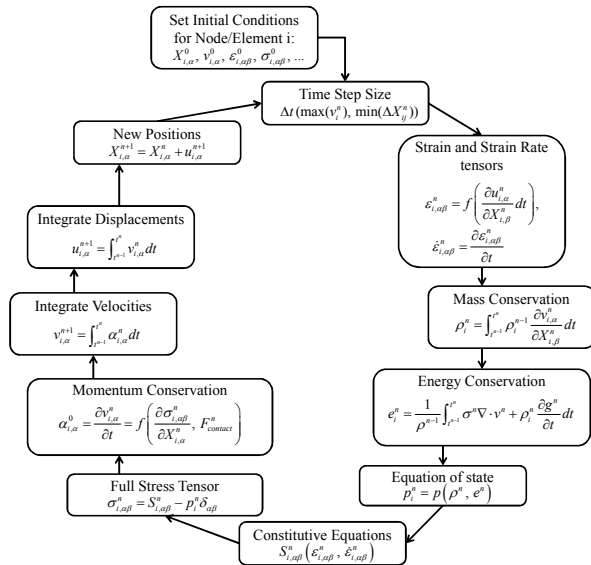


Fig. 1. Finite element solution procedure (see Ref. [9] for the detail descriptions).

18]. Among the various computational codes for wound ballistics, this research adopts the AUTODYN hydrocode to solve the mass conservation equation, the energy conservation equation, and the Equation of state (EOS), as shown in Fig. 1 [9]. For the sake of accurate simulation, the material properties for the ballistic gelatin and bullet should be inserted accurately; however, these show a large variance. Thus, in this section, the FE simulation and our measurements of the involved material properties are described.

2.1 Material model of ballistic gelatin block

The numerical simulation of high-speed impact on the ballistic gelatin, whose behavior is similar to that of human tissue without bone or skin, is a very difficult subject. The ballistic gelatin can be modeled as a viscoelastic material whose shear modulus is rate-dependent and whose local behaviors under high-speed impact become that of a liquid or gas.

In the literature, the rate-dependent stress-strain relationship has been tested in many ways [19–22], including the Hopkinson bar test, which utilizes the velocity of sound in the material, as shown in Fig. 2 [23]. Although this method is a standard measurement, conducting these experiments for a wide range of velocities at our institute is difficult.

For more accurate FE simulation, we should adopt a mechanical model of the rate-dependent material properties. Basically, the material models should be accurate enough to predict the behavior of the ballistic gelatin but simple enough to calculate its behavior in a reasonable amount of time. Until now, many theories and approaches have been developed; in this research, the Equation of state (EOS), the Johnson-Cook failure model, and the viscoelastic material model are employed for the rate-dependent bulk modulus and the rate-dependent shear modulus [24]. In our study, we use the Mie

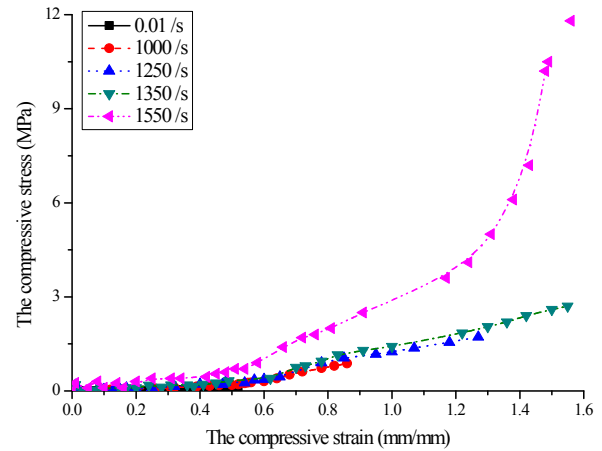


Fig. 2. Strain rates of 10% ballistic gelatin at high deformation rates (Redrawn from Ref. [23]).

Gruneisen equation of state as the equation of state and the Johnson-Cook failure model as the failure model. As stated, we employed the most commonly used material properties that have been published in the literature, with the exception of the rate-dependent shear moduli of gelatin blocks with different concentrations. In this research, these shear moduli are measured by indentation tests or by stress-relaxation tests.

2.1.1 Equation of state (EOS)

The equation of state is the equation used for the hydrodynamic prediction of a solid material. Without shear stress or force, the pressure inside a gas or fluid is only dependent on the density and the internal energy. In this scenario, the equation of state is used to calculate the magnitude of the pressure. When a solid material is under high-speed deformation, it behaves like a gas or fluid, and the internal pressure of the solid material can be calculated with the equation of state. Because ballistic gelatin deforms rapidly, the Mie-Gruneisen EOS is used. The Mie-Gruneisen EOS is the Taylor approximation of the state surface of the measured Hugoniot curve, and it is known that this EOS cannot predict phase changes [23]. With the Mie-Gruneisen EOS, the internal pressure is determined with respect to the volume and the internal energy in the hydrocode (AUTODYN) [24].

2.1.2 Johnson-cook failure model

To address the rate-dependent failure mode, this research adopts the Johnson-Cook failure model as follows:

$$D = \sum \frac{\Delta \epsilon}{\epsilon^f} \quad (1)$$

$$\epsilon^f = \left[D_1 + D_2 e^{D_3 \sigma^*} \right] \left[1 + D_4 \ln \left| \dot{\epsilon}^* \right| \right] \left[1 + D_5 T^* \right] \quad (2)$$

$$D_1 = -0.135490, D_2 = 0.601496, \quad (3)$$

$$D_3 = 0.258923, D_4 = 0.030127, D_5 = 0$$

where the effective failure strain is denoted as ϵ^f . The nor-

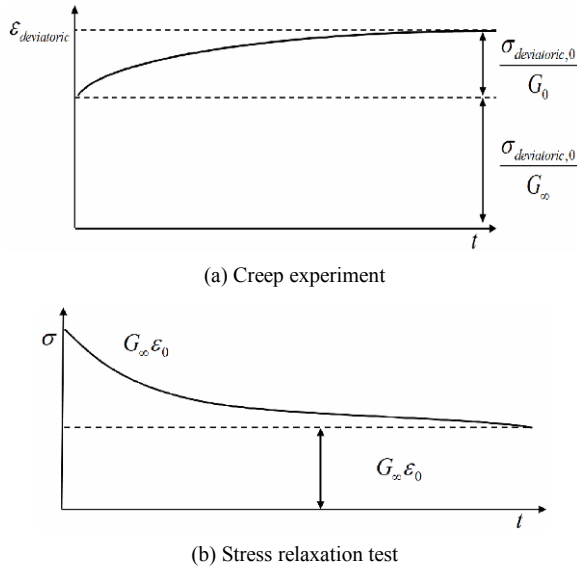


Fig. 3. Experiments for determining the coefficients of a viscoelastic material: (a) creep response to the initial stress σ_0 ; (b) the stress relaxation test due to the initial strain ε_0 (The deviatoric stress and the deviatoric strain are denoted as $\sigma_{deviatoric}$ and $\varepsilon_{deviatoric}$, respectively.).

malized effective plastic stress and rates are denoted as σ^* and $\dot{\varepsilon}^*$, respectively. The normalized temperature is T^* . The involved constants D_1 , D_2 , D_3 , D_4 , and D_5 can be obtained by Hopkinson-bar or Taylor-bar tests. From the literature, these constants are set by ignoring the effect of temperature in this research [24].

2.1.3 Rate-dependent shear modulus

It is known that many polymers, such as gelatin, rubber and plastic, often behave as elastic materials, viscous materials, or a combination of the two. Thus, the ballistic gelatin considered here is modeled as a viscoelastic material showing altered stress and strain curves under altered loading conditions. From a mechanical energy point of view, the viscoelastic material dissipates the internal energy with respect to time. To model the viscoelastic material properties, various finite element models have been proposed. In our numerical simulation, the Kelvin model and the Maxwell model are combined, as implemented in AUTODYN. Note that determining the coefficients in the viscoelastic material model is an issue that must be solved. One of the conventional models conducts creep experiments and measures the relaxed strain with respect to time, as shown in Fig. 3(a). Another method is the stress relaxation method, which measures the stress value with respect to time to compute the involved constants, as shown in Fig. 3(b).

By combining the Kelvin model and the Maxwell model, the shear modulus G becomes time dependent, as follows:

$$G(t) = G_v e^{-\beta t}, \quad \beta = \frac{G_0 - G_\infty}{\eta}, \quad G_v = G_0 - G_\infty \quad (4)$$

where the instantaneous shear modulus and the long-term shear modulus are denoted as G_0 and G_∞ , respectively. The decay constant is denoted as β . From the literature, it has been shown that the involved constants are highly dependent on the manufacturing environments [25–28]. Therefore, to have consistent viscoelastic material properties, we made 10% gelatin blocks. Indentation and stress relaxation experiments were conducted.

2.2 Indentation test for shear modulus

The spherical indentation test measures the change of the reaction force with respect to time when a spherical indenter is lowered into a viscoelastic material, as shown in Fig. 4(a) [25, 29]. The rate-dependent material properties are measured for different gelatin concentrations. In our research, we adopt the experimental setup shown in Fig. 4(b).

To measure the rate-dependent material properties, the polished stainless ball probe is first lowered down to a 10% gelatin block with a certain indentation length and the probe is fixed, as shown in Figs. 4(a) and 4(c). While maintaining this status, the reaction forces from the gelatin block to the probe are measured for a sufficient period of time. A standard measured force is given in Fig. 4(d). Because the probe is lowered with a constant speed, it can be observed that the reaction force proportionally increases up to 50 gf (Fig. 4(d)). When the probe is fixed, due to the stress relaxation in the viscoelastic material, the magnitude of the reaction force decreases, as shown in Fig. 4(d). The mathematical function to fit the section of the reaction force after it has been fixed is constructed with the Eq. (5). The parameters are inserted into Eqs. (6) and (7) to obtain the rate-dependent shear modulus [25–28]. In these equations, the maximum indentation length of the probe is denoted as h_{\max} and the time when the stress relaxation starts is denoted as t_R .

$$P(t) = (B_0 + \sum_{i=1}^3 B_i e^{-\frac{t}{\tau_i}}) \quad (5)$$

$$C_i = \frac{B_i}{\beta_i h_{\max}^2 (8\sqrt{R}/3)}, \quad \beta_0 = 1, \quad (6)$$

$$\beta_i = \frac{\tau_i}{t_R} (e^{t_R/\tau_i} - 1), \quad i > 0$$

$$G(t) = \frac{1}{2} (C_0 + \sum_{i=1}^3 C_i e^{-\frac{t}{\tau_i}}). \quad (7)$$

After arriving at Eq. (7), we obtain the parameters used for the FE hydrocode (AUTODYN) with Eq. (8).

$$G(t) = G_\infty + (G_0 - G_\infty) e^{-\beta t} \quad (8)$$

where G_0 is the instantaneous shear modulus, G_∞ is the long-term shear modulus, and β is the viscoelastic decay constant. The values obtained using the above indentation test (Fig. 4) for a 10% gelatin block are shown in Table 1. These obtained values are used in the viscoelastic material model.

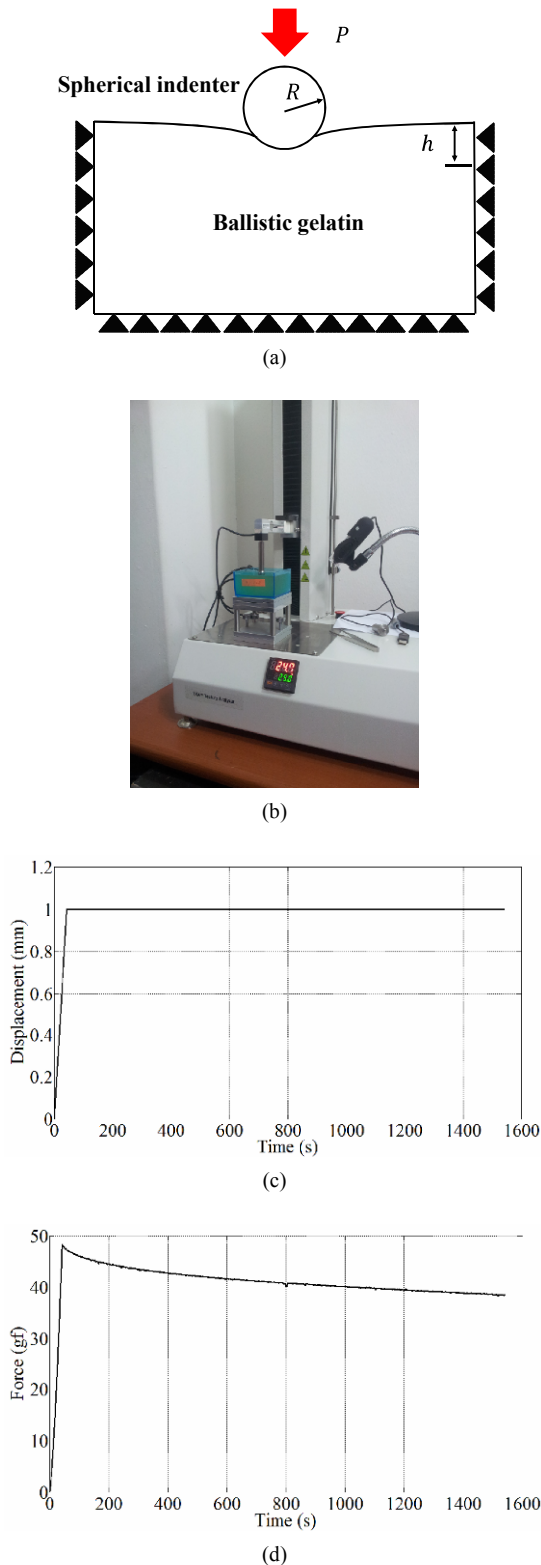


Fig. 4. Spherical indentation test: (a) diagram of spherical indentation test on the gelatin sample (P : reaction force on the indenter, R : radius of spherical indenter, and h : displacement of indenter from the surface of the gelatin sample); (b) test machine used for indentation test; (c) measure of displacement of indenter with time; (d) measure of force on the indenter with time.

Table 1. The instantaneous shear modulus, long-term shear modulus, and decay constant.

G_0	G_∞	β
21427.41 Pa	15818.91 Pa	0.00087

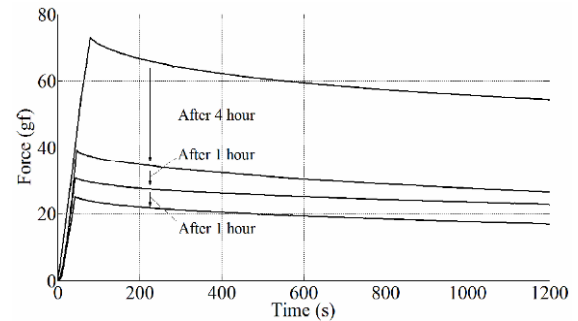


Fig. 5. Spherical indentation test according to the aging time (10% ballistic gelatin block).

2.2.1 Effect of preparation time and temperature increase

To prevent both ice formation and liquidation from adversely affecting the material properties of the ballistic gelatin, to ensure that its material properties are similar to that of a human body, its temperature should be maintained between 0°C and 10°C . However, because the real firing tests are conducted at normal room temperature, degradation of the material properties of the ballistic gelatin block should be considered and controlled if possible [19]. In our preparation, the gelatin blocks are kept inside ice boxes before transportation to the experiment site. Experimental setup usually took one or two hours. Even though the exposure time to the hot light source for the high-speed camera is short, the temperature increase caused by the heat from the light source cannot be ignored. To show this effect on material degradation, Fig. 5 shows the recorded reaction forces at a depth of 2 mm at different time intervals; in Fig. 4, the reaction forces are measured with 1-mm-deep indentations. The first indentation test shows 73 gf for the maximum reaction force. After 4 h have passed, another indentation test shows that the maximum reaction force decreased to 39 gf; degradation of the material strength can be clearly seen in subsequent indentation tests. This experiment illustrates that the rising temperature and the increased aging time inevitably cause degradation of the material properties; this is one of the sources of the chaotic experimental results that we obtained.

2.3 Finite element modeling and applied material properties for impact simulation

2.3.1 Modeling of gelatin block

Many hydrocodes that can simulate high-speed impact have been developed. Among them, this research uses the AUTODYN hydrocode with the above finite element theory. The finite element model is constructed with the ballistic

Table 2. Material properties of the 10% gelatin block.

Density, ρ	Viscoelasticity					
	Instantaneous shear modulus, G_0	Shear modulus, G_∞	Viscoelastic decay constant, β			
1030 kg/m ³	0.214 MPa	0.158 MPa	0.00087 s ⁻¹			
Mie-Gruneisen EOS (Shock EOS linear)						
Gruneisen coefficient	c_1	s_1	s_2			
0.17	1553 m·s ⁻¹	1.93	0 s·m ⁻¹			
Johnson-Cook failure model						
D_1	D_2	D_3	D_4	D_5	Melting temperature	Reference strain rate
-0.13549	0.6015	0.25892	0.030127	0	20°C	0.001

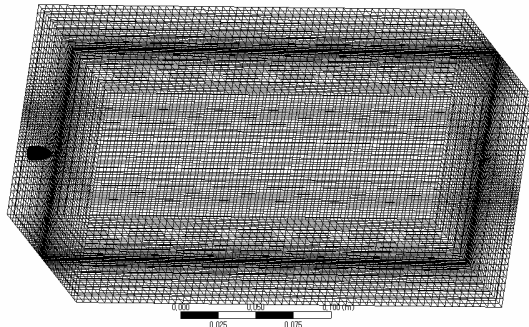


Fig. 6. Finite element model for ballistic gelatin block and bullet.

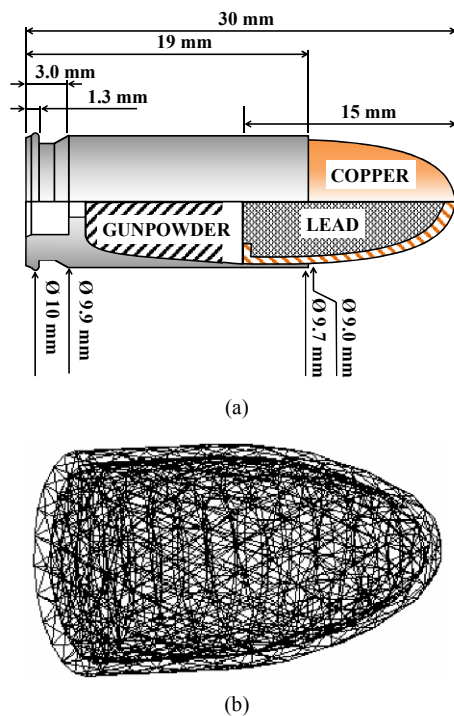


Fig. 7. Modeling of 9 mm × 19 mm parabellum bullet: (a) bullet profile sketch; (b) finite element mesh.

gelatin block and the bullet is modeled as a 9 mm × 19 mm parabellum bullet. The size of the gelatin block is 30 cm 15 cm 15 cm. The finite element meshes of the bullet and the gelatin block are shown in Fig. 6.

Table 3. Material properties of the bullet interior (Lead).

Density, ρ	Steinberg Guinan strength		Shear modulus
	Initial yield stress	Maximum yield stress	
1134 kg/m ³	8 MPa	0.1 GPa	11.13 GPa
Shock EOS linear			
Gruneisen coefficient	c_1	s_1	s_2
2.74	2006 m·s ⁻¹	1.429	0 m·s ⁻¹

Table 4. Material properties of the bullet coating (Copper).

Density, ρ	Bilinear isotropic hardening		Shear modulus
	Yield strength	Tangent modulus	
8900 kg/m ³	70 MPa	2 GPa	46.4 GPa
Gruneisen coefficient	c_1	s_1	s_2
2	3958 m·s ⁻¹	1.497	0 m·s ⁻¹

The material properties for the 10% gelatin block used in the AUTODYN hydrocode are illustrated in Table 2. As stated, the material properties of the ballistic gelatin block are measured by the indentation test and the other material properties are taken from the Refs. [30–32].

2.3.2 Modeling of bullet

The sketch and finite element mesh for the 9 mm 19 mm parabellum bullet are given in Fig. 7. The internal part of the bullet is filled with lead and the outer surface is coated with copper [33].

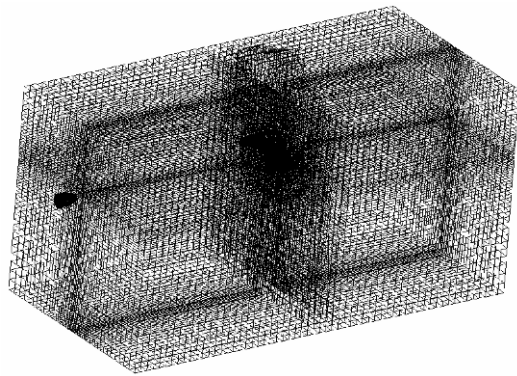
The elasto-plasticity material model is used for the bullet in Tables 3 and 4. Strictly speaking, the bullet should also be modeled considering the high-speed impact behavior. Because the rigidity of the bullet is sufficiently high, the elasto-plasticity material model is employed [33, 34].

2.3.3 Modeling of cow bone

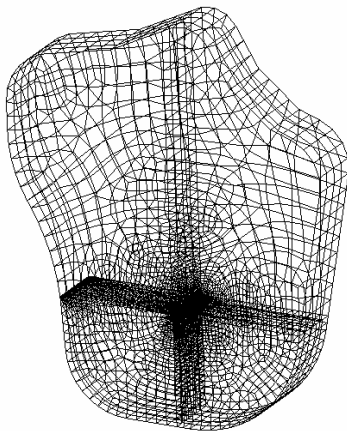
As stated in the introduction, one of our goals is to investigate the mechanical behavior of bone under high-speed impact. To our knowledge, there has been some research that

Table 5. Material properties of cow bone.

Density, ρ	Viscoelasticity			Bulk modulus
	Instantaneous shear modulus, G_0	Shear modulus, G_∞	Viscoelastic decay constant, β	
2000 kg/m ³	0.675 MPa	0.5 MPa	0.1 s ⁻¹	6 GPa
Principal strain failure				
Maximum principal strain, ε_{\max}			Maximum shear strain, γ_{\max}	
0.5			0.5	



(a)

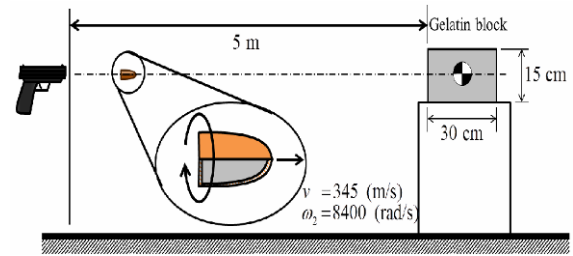


(b)

Fig. 8. Finite element model of gelatin block with bone: (a) position of bone; (b) shape of bone.

has considered bone under high-speed impacts [10]. As an extension, our research conducted some experiments with gelatin blocks and bone. The bone is modeled, as shown in Fig. 8, and inserted into the upper portion of the gelatin block.

Some static failure models of bone can be found in the Ref. [35], but it is rare to find studies that investigate the dynamic failure of bone. Therefore, we inversely obtained the material properties after comparing the finite element results with the experimental results; the experimental results are presented in a later portion of this paper. The cow bone is modeled with a viscoelastic material model with a high stiffness value, as shown in Table 5.



(a)



(b)

Fig. 9. Experiment setup for gelatin blocks: (a) schematic illustration; (b) real experiment.



(a)



(b)



(c)

Fig. 10. Gelatin blocks: (a) gelatin block without cow bone; (b) with cow bone; (c) the high-speed camera and a lamp.

3. High-speed impact experiments

3.1 Experiment

To study the rapid deformation in wound ballistics, this section presents our experimental and computational results; due to the regulations of the ministry of military of the Republic of Korea for the ballistic experiment, only Sig Saure P226, which is commercially available, is used for the following experiments (Fig. 9). A trained shooter shoots the gelatin blocks from a distance of 5 m, as shown in Fig. 9.

In these experiments, 15 cm × 15 cm × 30 cm gelatin blocks with and without cow bone and nerve fibers are prepared, as shown in Figs. 10(a) and 10(b) [36]. A high-speed camera,

shown in Fig. 10(c), is installed at the sides of the gelatin blocks.

In order to capture the high-speed rate deformation before and after impact, a high-speed camera with more than 10,000 frames per second is installed. Considering the recoding time related to the memory and resolution of our high-speed camera, a shutter speed of 13029 frames per second is set. After the bullet's impact, most of the kinetic energy of the bullet is dissipated by deforming and tearing up the ballistic gelatin block and we can observe both temporary and permanent cavities. The evolving shapes of temporary cavities can be captured and investigated by the high-speed camera. However, it is difficult to precisely examine the remaining shapes of the permanent cavities. Normally, to examine the shapes of a permanent cavity, the ballistic gelatin blocks are cut after ballistic testing. Unfortunately, this inevitably distorts the shapes of the cavities. To overcome this limitation in our study, the shapes of permanent cavities are instead scanned by an industrial CT (Computed tomography) and three-dimensional CAD models of the permanent cavities are built with the scanned CT images.

3.2 Ballistic gelatin experiment 1

For the first experimental and computational tests, the instantaneous images of the pure ballistic gelatin blocks before and during the ballistic collision are captured; the FE results are compared with these images. It should be mentioned that the quantitative analysis between the experiment and the finite element simulation is almost impossible due to the chaotic behavior of the bullet. However, the qualitative analysis that is performed here and the deformation tendencies of the wounds in the gelatin blocks are similar to each other.

Investigating the images taken with our high-speed camera (at 13029 frames per second) reveals that, before collision, the bullet moves toward the block of ballistic gelatin at 21 mm per frame; this is equivalent to a bullet speed of 313 m/s. The time for the bullet to pass through the block of ballistic gelatin is about 0.0012 seconds in the experiment, whereas the simulation predicted a time of 0.0017 seconds. In our experiment, the decelerated speed of the bullet after the passing through is impossible to measure because the bullet is covered with deformed gelatin debris. It is also observed that the approximate incident angle between the bullet and the surface of the gelatin block is 3 degrees.

Some images taken before, during, and after the impact and the collision are shown in Fig. 11. Just after impact, there are temporary cavities and a permanent cavity inside the ballistic gelatin block. The images taken as the bullet is passing through the block show that the bullet experiences immediate deceleration and that the ballistic gelatin block at the impact surface flows away from the bullet to form a pulsating temporary cavity. In Fig. 12, the evolving diameters of the temporary cavities in this experiment and the finite element simulation are compared to each other. This comparison

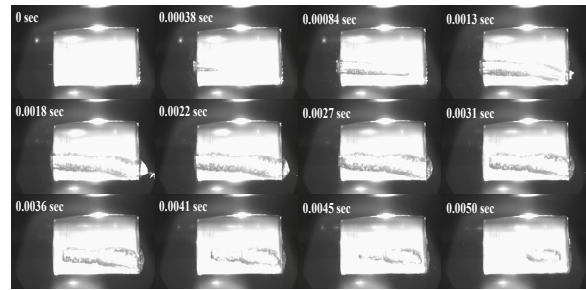


Fig. 11. High-speed camera images taken during impact (13029 frames/ second, model: Phantom V7.3).

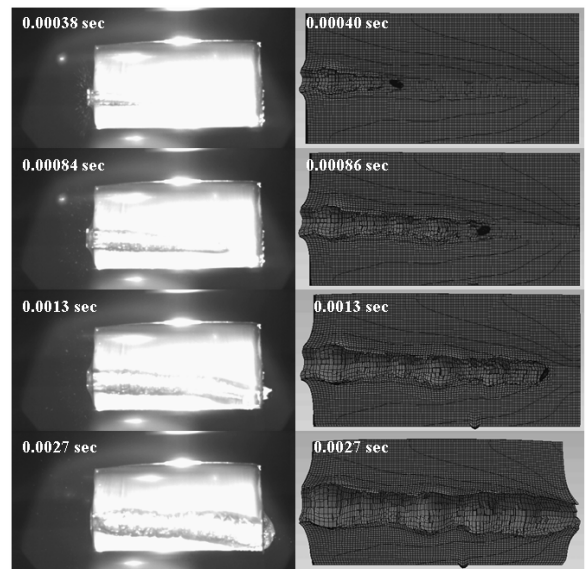
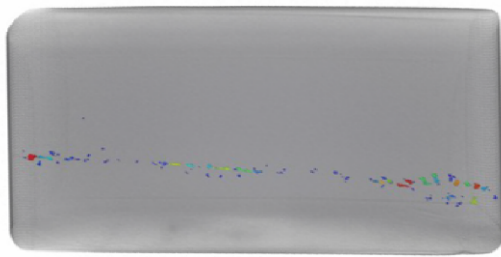


Fig. 12. Comparisons of the deformations from the experiment and the finite element simulation.

reveals that nearly-identical behavior can be predicted by the FE procedure; without the Johnson-Cook failure model, the pulsations of the temporary cavities cannot be obtained. Furthermore, it is expected that the gelatin undergoes some rotational motion due to the centrifugal force exerted on the ballistic gelatin by the rotation of the bullet. In this experiment, it was difficult to observe this rotational motion. After the temporary cavity reaches maximum volume, it contracts due to the restoring force of the ballistic gelatin. Qualitatively, the contraction behaviors of the temporary cavities of the experiment and the FE simulation are similar to each other. Yawing phenomena caused by the resistance force from the ballistic gelatin block are also observed. Normally, the resistance forces from the ballistic gelatin block cause bending and compressive stresses on the surface of the bullet, which can compress it or even cause it to fracture. However, inside the pure ballistic gelatin block, the bullet (9 mm 19 mm parabellum bullet) maintains its shape and undergoes only minor changes in form and loses no mass: these are shape-stable bullets. It is observed that the translation and rotation kinetic energies of the bullet cause the dramatic deformations

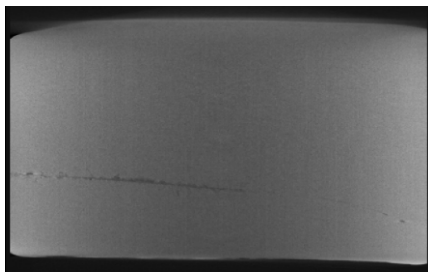


(a)

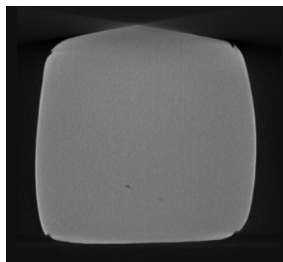


(b)

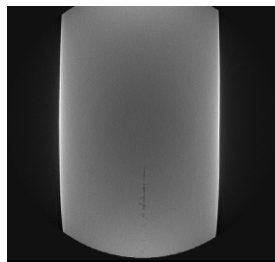
Fig. 13. (a) Permanent cavity after penetration; (b) a three-dimensional CAD model based on the industrial CT images.



(a)



(b)



(c)

Fig. 14. (a) Side CT image; (b) front CT image; (c) top-view CT image of the penetration scene.

seen inside of the ballistic gelatin block.

Fig. 13(a) shows the permanent cavity inside the ballistic gelatin block. In order to examine the shape of the permanent cavity, blocks are typically dismantled and the remaining shape is investigated. However, in our study, an industrial CT machine is utilized to take snapshots of inside the gelatin block. With the help of automated CAD software, it was possible to construct a three-dimensional model, as shown in

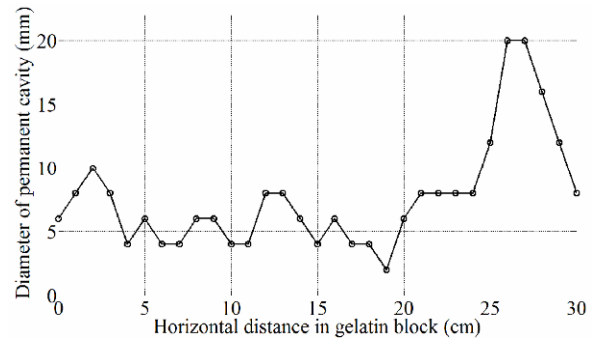


Fig. 15. Permanent cavity diameter with the position in the gelatin block obtained by CT.

Fig. 13(b).

3.3 Ballistic gelatin experiment 2

For the next study, we installed the cow bone and nerve fiber, whose material properties are similar to those of human bone and nerve fiber, inside the 10% ballistic gelatin block. Note that the behavior of a projectile during high velocity impact with a purely viscoelastic medium is largely governed by the density of the medium. From a physical point of view, the higher the density of the ballistic gelatin block, the greater the pressure acting at the nose of the bullet. This causes the swirling and tumbling motion of the bullet. Additionally, some weaker parts of the bullet are often squeezed out and shattered. For these reasons, pure gelatin blocks are less than ideal because they do not have blood vessels, nerve fibers, and/or bones embedded in them. To overcome this limitation, we installed cow bones and nerve fibers into the gelatin blocks and conducted both FE simulation and experiments. The same experimental procedures used for the pure gelatin blocks were followed.

Fig. 16 shows some images taken while the bullet was passing through the gelatin block. Although an experienced shooter is firing the gun, some detailed impact conditions, such as the incident angle, the position, and the impact speed, are different between each experiment. Furthermore, the material properties of the bone and nerve fiber are arbitrarily chosen; as such, the FE result exhibits a large discrepancy with the experimental result. By analyzing the images of the bullet, it was found that the bullet speed before impact is about 313 m/s and that the measured time of the bullet's passing through the gelatin block is about 0.0012 seconds. However, the FE simulation in Fig. 17 shows that the time for the bullet to pass through the block is 0.0014 seconds; this discrepancy is partially caused by the erroneous material properties of the bone and nerve fiber, the fracture, and the pulverization of the

bone debris. Additionally, the first and the second experiments confirm that the motion of the bullet is influenced primarily by the density, viscosity, and flowability of the medium it is passing through. One of the observed differences between the first and second tests is that a secondary cavity appears near the bone around 0.0038 s and around 0.0046 s.

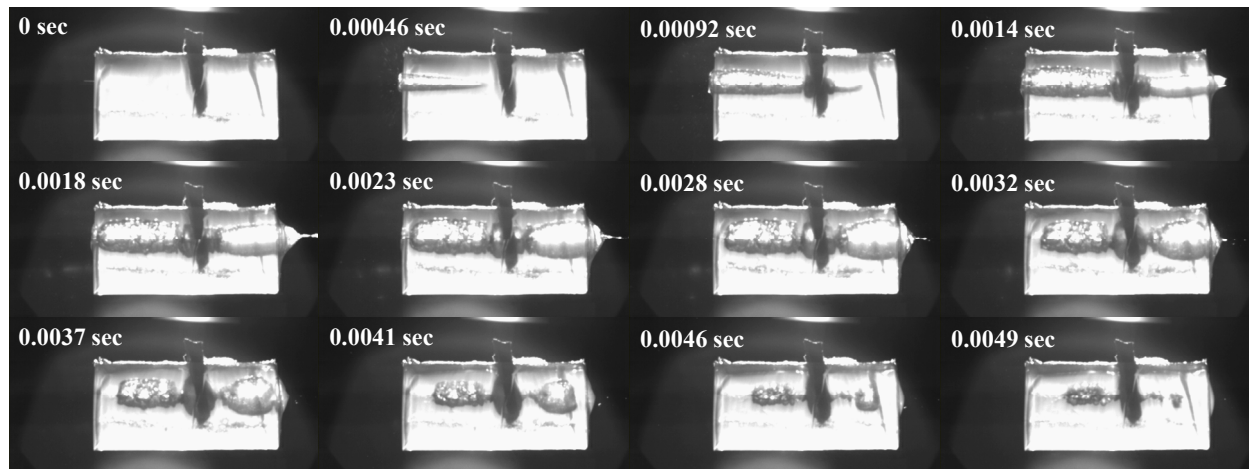


Fig. 16. Penetration scenes of gelatin block with cow bone and nerve fiber taken by high-speed camera (FPS: 13029 frames/second; an impact velocity 313 m/s).

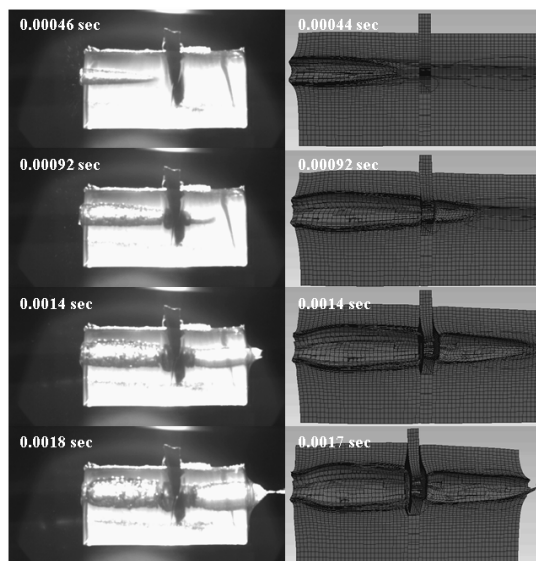


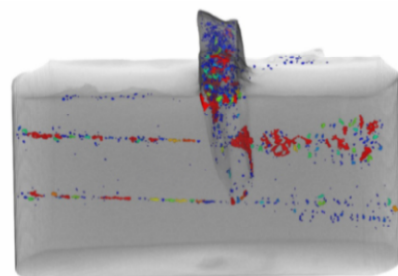
Fig. 17. High-speed camera image and finite element simulation results.

This secondary cavity is also observed in the FE simulation. When the bullet passes through the bone, the size of the temporary cavity behind the bone is observed to become smaller. This is partially due to the energy dissipation of the bullet by the bone. Because the reaction force of the bone is larger than that of the ballistic gelatin block, the bullet undergoes a larger rotation, which increases the size of the permanent cavity.

After the experiment, the three-dimensional CT is also applied to construct the three-dimensional CAD model (without the destruction of the ballistic gelatin block), as shown in Figs. 18 and 19; here, it should be noted that there are the two permanent cavities in Fig. 18. After the first shot, the shooter fired a secondary shot. Fig. 18(c) shows the fracture of the bone and nerve fiber. The investigation of the bone and nerve fiber shows the sliding and separation between



(a)



(b)



(c)

Fig. 18. (a) Permanent cavity inside the gelatin block and the cow bone after the impact; (b) penetration scene taken by CT; (c) the fracture of the bone.

the bone and the nerve due to the differences in their strengths. This is also an important aspect that should be considered in the treatment of wounds and bone infection.

Fig. 20 shows the diameter variation of the permanent

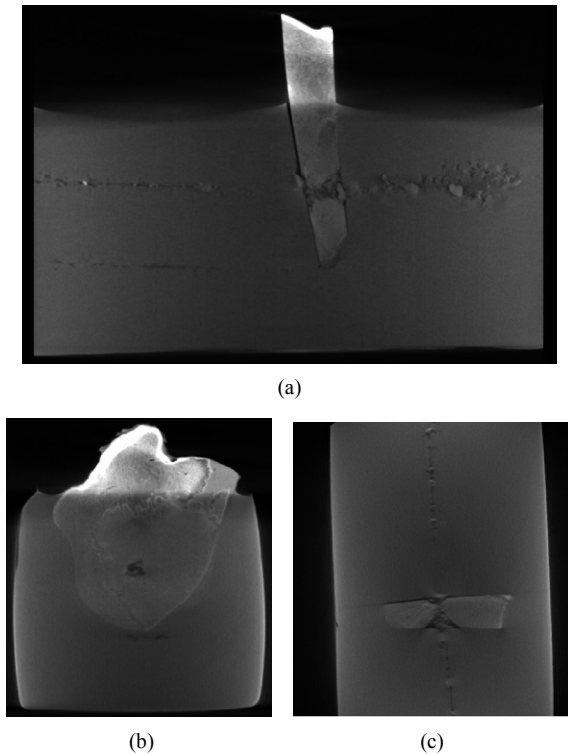


Fig. 19. CT images at the: (a) side; (b) front; (c) top-view of the penetration scene.

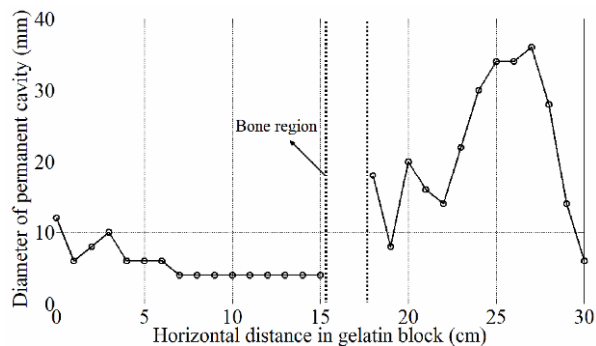


Fig. 20. Permanent cavity diameter as a function of the position in the gelatin block.

cavity in the ballistic gelatin block. The first cavity collapses after a few milliseconds because some of the bullet's energy is converted into the kinetic energy of the ballistic gelatin block. Next, a secondary cavity is created; the size of the secondary cavity is smaller than that of the first cavity because less kinetic energy is available. This process creates so-called cavity pulsation, which occurs between 0 cm and 10 cm in Fig. 20.

4. Conclusions

To understand and analyze the damage caused in the human body due to high-speed impact, this research conducted experimental and computational investigations for bullet

penetration into viscoelastic ballistic gelatin blocks. The computational investigations are based on the explicit finite element analysis AUTODYN. For the computational models for the viscoelastic gelatin material, metal, and bone, rate-dependent nonlinear material models are employed. To obtain the viscoelastic shear modulus, this study uses an in-house indentation test facility and measurement software. In order to conduct qualitative studies, some experiments (following domestic regulations) were conducted. During and after the experiments, the ballistic gelatin blocks with and without bone are scanned with a three-dimensional CT and 3-D CAD models are constructed to analyze the shapes of the permanent cavities. By comparing the computational results and the experiment results, qualitatively similar results in terms of the shape of the temporary and permanent cavities and the shockwave propagations can be obtained. However, because the experiments are statically stochastic, comparison of the quantitative results is impossible.

To consider how the presence of bone and nerve fiber affect the high-speed impact, a cow bone is placed inside the ballistic gelatin block. It is observed that just after direct impact on the bone, another shockwave at the surface of the bone is generated. This shockwave causes another cavity, in addition to the primary cavities, along the direction of the bullet's penetration. Furthermore, the retardation becomes serious and causes the bullet to swirl and tumble. This shockwave also cracks and damages the nerve and bone. Delamination, i.e. a mode of failure between the nerve and bone, is also observed. Because the instantaneous kinetic energy of the bullet is decreased significantly after impact inside the ballistic gelatin block, which has a higher retardation coefficient, the bullet dramatically swirls and tumbles inside the ballistic gelatin block. This induces a bigger permanent cavity that is approximately twice as large compared to the scenario without bone impact.

This research investigates the high-speed penetration of a bullet in a 10% ballistic gelatin block with and without bone. Although this type of research has been conducted for many decades, these tests do not typically consider both the computational and experimental results. Particularly, because the failure modes of viscoelastic gelatin, brittle bones, and ductile bullets are very different from each other, a full-scale, reliable computational model is still very difficult to build. Improving the FE prediction accuracy was not attempted here; this should be researched in the near future. In conclusion, the current study can be used to design new protective devices or systems for humans or to improve current devices/systems by estimating their abilities to reduce the damage caused by the high-speed impacts.

Acknowledgement

This work was supported by the Research fund of Survivability Technology Defense Research Center of Agency for Defense Development of Korea (No. UD120019OD).

References

- [1] G. Seisson, D. Hebert, L. Hallo, J. M. Chevalier, F. Guillet, L. Berthe and M. Boustie, Penetration and cratering experiments of graphite by 0.5-mm diameter steel spheres at various impact velocities, *Int. J. Impact Eng.*, 70 (2014) 14-20.
- [2] N. Ndompetelo, P. Viot, G. Dyckmans and A. Chabotier, Numerical and experimental study of the impact of small caliber projectiles on ballistic soap, *J. Phys. IV*, 134 (2006) 385-390.
- [3] C. C. Shi, M. Y. Wang, J. Li and M. S. Li, A model of depth calculation for projectile penetration into dry sand and comparison with experiments, *Int. J. Impact Eng.*, 73 (2014) 112-122.
- [4] B. Akers and A. Belmonte, Impact dynamics of a solid sphere falling into a viscoelastic micellar fluid, *J. Non-Newton Fluid*, 135 (2-3) (2006) 97-108.
- [5] D. J. Frew, M. J. Forrestal and J. D. Cargile, The effect of concrete target diameter on projectile deceleration and penetration depth, *Int. J. Impact Eng.*, 32 (10) (2006) 1584-1594.
- [6] E. Sevkatev, Experimental and numerical approaches for estimating ballistic limit velocities of woven composite beams, *Int. J. Impact Eng.*, 45 (2012) 16-27.
- [7] M. G. Perdekamp, S. Pollak, A. Thierauf, E. Strassburger, M. Hunzinger and B. Vennemann, Experimental simulation of reentry shots using a skin-gelatine composite model, *Int. J. Legal Med.*, 123 (5) (2009) 419-425.
- [8] A. Dorogoy, D. Rittel and A. Brill, Experimentation and modeling of inclined ballistic impact in thick polycarbonate plates, *Int. J. Impact Eng.*, 38 (10) (2011) 804-814.
- [9] S. Hiermaier, *Structures under crash and impact : continuum mechanics, discretization and experimental characterization*, Springer, New York, USA (2008).
- [10] B. Kneubuehl, *Wound ballistics: Basics and applications*, Springer (2011).
- [11] S. Yang, A. Fafitis and A. Wiesel, Nonlinear impact model of a tennis racket and a ball, *J. Mech. Sci. Technol.*, 26 (2) (2012) 315-321.
- [12] Y. Kim, J. Yoo and M. Lee, Optimal design of spaced plates under hypervelocity impact, *J. Mech. Sci. Technol.*, 26 (5) (2012) 1567-1575.
- [13] Y. F. Deng, W. Zhang, Y. G. Yang, L. Z. Shi and G. Wei, Experimental investigation on the ballistic performance of double-layered plates subjected to impact by projectile of high strength, *Int. J. Impact Eng.*, 70 (2014) 38-49.
- [14] M. V. Swain, D. C. Kieser, S. Shah and J. A. Kieser, Projectile penetration into ballistic gelatin, *J. Mech. Behav. Biomed.*, 29 (2014) 385-392.
- [15] L. Liu, Y. R. Fan and W. Li, Viscoelastic shock wave in ballistic gelatin behind soft body armor, *J. Mech. Behav. Biomed.*, 34 (2014) 199-207.
- [16] F. Bresson, J. Ducouret, J. Peyre, C. Marechal, R. Delille, T. Colard and X. Demondion, Experimental study of the expansion dynamic of 9 mm Parabellum hollow point projectiles in ballistic gelatin, *Forensic Sci. Int.*, 219 (1-3) (2012) 113-118.
- [17] Y. K. Wen, C. Xu, H. S. Wang, A. J. Chen and R. C. Batra, Impact of steel spheres on ballistic gelatin at moderate velocities, *Int. J. Impact Eng.*, 62 (2013) 142-151.
- [18] I. Ionescu, J. E. Guilkey, M. Berzins, R. M. Kirby and J. A. Weiss, Simulation of soft tissue failure using the material point method, *J. Biomech. Eng-T Asme*, 128 (6) (2006) 917-924.
- [19] D. S. Cronin and C. Falzon, Characterization of 10% Ballistic Gelatin to Evaluate Temperature, Aging and Strain Rate Effects, *Exp. Mech.*, 51 (7) (2011) 1197-1206.
- [20] J. Kwon and G. Subhash, Compressive strain rate sensitivity of ballistic gelatin, *J. Biomech.*, 43 (3) (2010) 420-425.
- [21] D. S. Cronin and C. Falzon, Dynamic characterization and simulation of ballistic gelatin, *Proceedings of the SEM Annual Conference*, Albuquerque New Mexico, USA (2009).
- [22] D. S. Cronin, C. P. Salisbury and C. R. Horst, High rate characterization of low impedance materials using a polymeric split Hopkinson pressure bar, *SEM Conference & Exposition on Experimental & Applied Mechanics*, St. Louis, Missouri (2006).
- [23] C. P. Salisbury and D. S. Cronin, Mechanical Properties of Ballistic Gelatin at High Deformation Rates, *Exp. Mech.*, 49 (6) (2009) 829-840.
- [24] ANSYS, *ANSYS AUTODYN User Manual*.
- [25] B. Qiang, J. Greenleaf, M. Oyen and X. M. Zhang, Estimating material elasticity by spherical indentation load-relaxation tests on viscoelastic samples of finite thickness, *Ieee T Ultrason Ferr*, 58 (7) (2011) 1418-1429.
- [26] M. L. Oyen, Spherical indentation creep following ramp loading, *J. Mater. Res.*, 20 (8) (2005) 2094-2100.
- [27] M. L. Oyen, Analytical techniques for indentation of viscoelastic materials, *Philos. Mag.*, 86 (33-35) (2006) 5625-5641.
- [28] J. M. Mattice, A. G. Lau, M. L. Oyen and R. W. Kent, Spherical indentation load-relaxation of soft biological tissues, *J. Mater. Res.*, 21 (8) (2006) 2003-2010.
- [29] X. M. Zhang, B. Qiang and J. Greenleaf, Comparison of the surface wave method and the indentation method for measuring the elasticity of gelatin phantoms of different concentrations, *Ultrasonics*, 51 (2) (2011) 157-164.
- [30] H. W. Kang, J. Kim, Y. Yu and J. Oh, Photoacoustic Response of Magnetic Nanoparticles to Pulsed Laser Irradiation, *J. Korean Phys. Soc.*, 55 (5) (2009) 2224-2228.
- [31] G. R. Johnson, Fracture characteristics of three metals subjected to various strains, strain rates, temperatures and pressures, *Engineering Fracture Mechanics*, 21 (1) (1985) 31-48.
- [32] M. Aihaiti and R. J. Hemley, *Equation of state of ballistic gelatin (II)*, 55048-EG.1, Carnegie Institute of Washington, DC (2011).
- [33] S. P. Mates and R. Rhorer, Dynamic deformation of copper-jacketed lead bullets captured by high speed digital image correlation, *Proceedings of the SEM Annual Conference*, Indianapolis, Indiana, USA (2010) 431-441.
- [34] D. S. Preece and V. S. Berg, Bullet impact on steel and Kevlar/steel armor-computer modeling and experimental data, *The Proceedings of the ASME Pressure Vessels and Piping Conference-Symposium on Structures Under Extreme Loading*, San Diego, CA, USA (2004).

- [35] V. Astier, L. Thollon, P. J. Arnoux, F. Mouret and C. Brunet, A finite element model of the shoulder for many applications: trauma and orthopaedics, *European HyperWorks Technology Conference*, Berlin, Germany (2007).
- [36] J. Jussila, Preparing ballistic gelatine - review and proposal for a standard method, *Forensic Sci. Int.*, 141 (2-3) (2004) 91-98.



Gil Ho Yoon received his B.S. degree in mechanical and aerospace engineering from Seoul National University in 1998. And he received his M.S. degree and Ph.D. in mechanical and aerospace engineering from Seoul National University in 2000 and 2004, respectively.

Dr. Yoon is currently an associate professor at School of Mechanical Engineering, Hanyang University, Seoul, Republic of Korea.



Ki Hyun Kim received his B.S. degree in mechanical engineering from Hanyang University in 2013.



Chung Hee Yoon received his B.S. degree in mechanical engineering from Hanyang University in 2013.



Jun Su Mo received his B.S. degree in mechanical engineering from Hanyang University in 2013.



Nam Hun Lim received his B.S. degree and M.S. degree in mechanical engineering from Hanyang University in 2012 and 2015, respectively.